ELSEVIER

Chemical Geology 184 (2002) 71–82

CHEMICAL GEOLOGY
INCLUDING
ISOTOPE GEOSCIENCE

www.elsevier.com/locate/chemgeo

Silica speciation in aqueous fluids at high pressures and high temperatures

Nikolay Zotov [a,b,*], Hans Keppler [a,c]

[a] *Bayerisches Geoinstitut, Universität Bayreuth, D-95449 Bayreuth, Germany*
[b] *Mineralogisch-Petrologisches Institut, Universität Bonn, D-53115 Bonn, Germany*
[c] *Mineralogisches Institut, Universität Tübingen, D-72074 Tübingen, Germany*

Received 29 August 2000; accepted 20 July 2001

Abstract

In-situ Raman measurements of silica speciation in aqueous fluids in equilibrium with solid quartz are reported to 14 kbar and 900 °C. Silica speciation in the fluid depends strongly on temperature and pressure. The Raman spectra indicate that below 600 °C and 6–8 kbar, only H_4SiO_4 monomers are present, while H_4SiO_4 monomers and $H_6Si_2O_7$ dimers coexist at higher temperatures and pressures. Above temperatures of about 850–900 °C and pressures of 12–13 kbar higher polymers may be present in significant concentrations. The enthalpy of the polymerization reaction $2H_4SiO_4 \leftrightarrow H_6Si_2O_7 + H_2O$ at 5 kbar pressure is $\Delta H = 12.6 \pm 1.3$ kJ/mol, while the reaction entropy is $\Delta S = 40.7 \pm 1.3$ J/mol K. The change of the molar volume of the solute $\Delta V_{sol} = V_{H_6Si_2O_7} - 2V_{H_4SiO_4}$ is virtually constant over the pressure and temperature range studied and equal to -39 ± 14 cm^3/mol.

Keywords: Silica speciation; Aqueous fluids; Diamond-anvil cell; Solubility; Raman spectroscopy; High pressure

1. Introduction

Silica is probably the most important solute in aqueous fluids in the Earth's crust and mantle. Accordingly, the solubility of SiO_2 polymorphs in water has been carefully studied over a wide range of pressures and temperatures (e.g. Anderson and Burnham, 1965; Fournier and Potter, 1982; Dove and Rimstidt, 1994; Manning, 1994). Early interpretations of experimental solubility data (see Walter and Helgeson, 1977) were based on the assumption that SiO_2 is present in aqueous solutions primarily as orthosilic acid monomers (H_4SiO_4). Accordingly, the reaction of solid SiO_2 with water is usually written as:

$$SiO_2(s) + 2H_2O(aq) \leftrightarrow H_4SiO_4(aq). \quad (1)$$

The equilibrium constant of reaction (1) depends strongly on pressure and temperature (Walter and Helgeson, 1977).

However, it is conceivable that orthosilic acid (H_4SiO_4) monomers are not the only species in the solution. Polymerized species, such as pyrosilicic acid ($H_6Si_2O_7$) dimers, could form according to reactions of the type:

$$2H_4SiO_4 \leftrightarrow H_6Si_2O_7 + H_2O. \quad (2)$$

Possible reaction pathways of reaction (2) have been proposed upon phenomenological considerations (Iler, 1979) and studied by quantum-chemical calcu-

* Corresponding author. Present address: Mineralogisch-Petrologisches Institut, Universität Bonn, D-53115 Bonn, Germany. Tel.: +49-228-732771; fax: +49-228-732770.
E-mail address: nzotov@uni-bonn.de (N. Zotov).

0009-2541/02/$ - see front matter
PII: S0009-2541(01)00353-9

lations on small molecular-like systems (Hench and West, 1990).

The silica speciation in alkaline and basic aqueous solutions has been studied in the past mainly by light scattering (Greenberg and Sinclair, 1955) and chromatographic separation (Dent Glasser and Lachowski, 1980). More recent studies using Raman and NMR spectroscopy have provided experimental evidence for the existence of silica polymers in alkaline solutions at ambient conditions (Earley et al., 1959; Freund, 1973; Alvarez and Sparks, 1985; Harris et al., 1980; Harris and Knight, 1983; Knight, 1988; Bass and Turner, 1997). At ambient pressure, the degree of polymerization in alkaline silicate solutions decreases with increasing temperature at least up to 180 °C (Busey and Mesmer, 1977; Kinrade and Swaddle, 1988).

Data on silica speciation in neutral solutions are even more scarce. Stumm and Morgan (1981) suggested that only monomer species exist in equilibrium with amorphous SiO_2. On the other hand, Cary et al. (1982) detected about 6% dimer species but no higher polymerized species in aqueous silica solutions using NMR spectroscopy. Polymerization of silicic acid molecules has been observed in molecular dynamics simulations (Feuston and Garofalini, 1990; Garofalini and Martin, 1994).

The abundance of polymerized species is expected to increase with increasing total silica concentration (Iler, 1979). Therefore, polymerized species are expected to be more abundant at higher pressures and temperatures where the silica solubility is very high. However, data for the actual silica speciation under these conditions are practically nonexistent.

We have recently published first results on the speciation of silica dissolved in water to 900 °C and 14 kbar by in-situ Raman spectroscopy in an externally heated diamond-anvil cell. The emphasis of this paper was on the identification of the observed Raman bands by comparison with calculated normal mode frequencies and Raman intensities. In the present paper we present numerous new experimental results, the *P,T* dependence of the H_4SiO_4 mode frequencies (Section 3.1) and provide further support of our band assignments by isotope substitution experiments. Moreover, we derive a thermodynamic model that describes silica speciation over a large range of pressures and temperatures.

2. Experimental

2.1. Diamond-anvil cell technique

All experiments were carried out with an externally heated Bassett-type diamond-anvil cell (Bassett et al., 1993). The cell utilizes two low-fluorescence type IIa diamonds of 0.21 carat with 1-mm culet faces cut parallel to (100). Iridium gaskets with 250-μm initial thickness and a 400-μm hole were used to contain the sample. Initial tests with rhenium gaskets proved to be unsatisfactory because of strong fluorescence of the aqueous fluid at high temperature, which is probably due to the dissolution of traces of rhenium. No fluorescence was observed with the iridium gaskets.

The cell is heated by molybdenum coils around the tungsten carbide seats which support the diamond anvils. Temperature is measured with two K-type thermocouples attached to the diamonds. The power of the upper and the lower heaters was controlled individually, which allows the temperature of each diamond to be kept constant to ± 5 °C during the experiments. Temperature was calibrated by visually observing the melting points of $NaNO_3$, CsCl, and NaCl inside the diamond cell at ambient pressure.

The charge loaded into the sample chamber usually consisted of 1–2 pieces of natural Brazilian quartz, high-purity water and a vapour bubble. The pressure was determined from the observed homogenization temperature (T_H) of the vapour bubble in conjunction with the equation-of-state of water proposed by Saul and Wagner (1989). The pressure determination is based on the assumption that the sample chamber behaves as an isochoric system after several cycles of heating and cooling (Bassett et al., 1993). The desired bulk density of water above T_H, and thus the desired pressure range, was approximately controlled by the initial size of the vapour bubble. In order to achieve very high pressures, experiments were also done without vapour bubble at the beginning.

During operation, the cell was flushed with an argon (98%)–hydrogen (2%) mixture to prevent oxidation of the diamonds and the molybdenum heaters. The maximum temperatures in the present experiments were limited to about 900–950 °C due to the necessity to use relatively long measuring times (at least 60 s) per spectral window in order to get reasonable signal-to-noise ratios.

2.2. Raman spectroscopy

The Raman spectra were recorded with two different Raman spectrometers (Spex 1874 and Dilor XY). In both cases the 514.5-nm line of an Coherent Innova 300 Ar^+ laser was used as excitation source operating at 2 ± 0.1 W power. Plasma lines were suppressed by an interference filter.

The Spex spectrometer was equipped with three 1800 gr/mm gratings and a Photonics charge-coupled device (CCD) detector cooled at liquid-N_2 temperature. Measurements were made in 155° scattering geometry using a beam expander and achromatic focussing lenses ($f = 56$ mm; N.A. = 3.1) for focussing the laser beam into the cell and for collecting the scattered radiation. The entrance slit width was 500 μm. Due to the large distance of the sample to the spectrometer entrance, accumulation times varied from 120 to 2000 s per spectral window (400 cm^{-1} width).

The XY spectrometer (800 mm focal length) was equipped with three 1800 gr/mm holographic gratings and a Spectrum-One back-thinned CCD detector cooled at liquid-N_2 temperature. Measurements were made in backscattering geometry under an Olympus microscope using a long-working distance objective LM Plan Fl 10X (N.A. = 0.25) in conjunction with confocal optics in front of the entrance slit. The XY spectrometer was operated in triple subtractive mode. The entrance slit width was 300 μm. A confocal hole of 200 μm was used in order to sample very small ($1-2$ μm^3) volumes in the chamber of the diamond cell, thus reducing the scattering contribution and black-body radiation from the diamonds and other parts of the cell. The black-body contribution measured at 900 °C is only 8% of the Raman signal from the solution and is nearly independent of frequency over the spectral window measured. Therefore, no correction for the black-body radiation was made. Accumulation times varied from 60 s above 800 °C to several minutes at lower temperatures. Data from different spectral windows (700 cm^{-1} width each) were processed using the Lab208 Dilor software. The Raman lines were fitted with pseudo-Voigt functions, which represent linear combination of Lorentzian and Gaussian components, in order to determine accurately the peak positions, the full width at half maximum (FWHM) and the integral intensities of the peaks. The frequency scale of the XY spectrometer was calibrated against the first-order Si phonon frequency.

3. Results and discussion

3.1. Low-pressure/low-temperature regime

Numerous Raman spectra of aqueous fluids in equilibrium with solid quartz were recorded with different bulk densities and at various temperatures. Some representative spectra are given in Figs. 1 and 2. A single peak at about 760–780 cm^{-1} is observed in the Raman spectra at temperatures below 500–800 °C and pressures below 6–8 kbar, depending on the bulk density of the individual experiment. Evidently, at these $P-T$ conditions only one kind of silica species

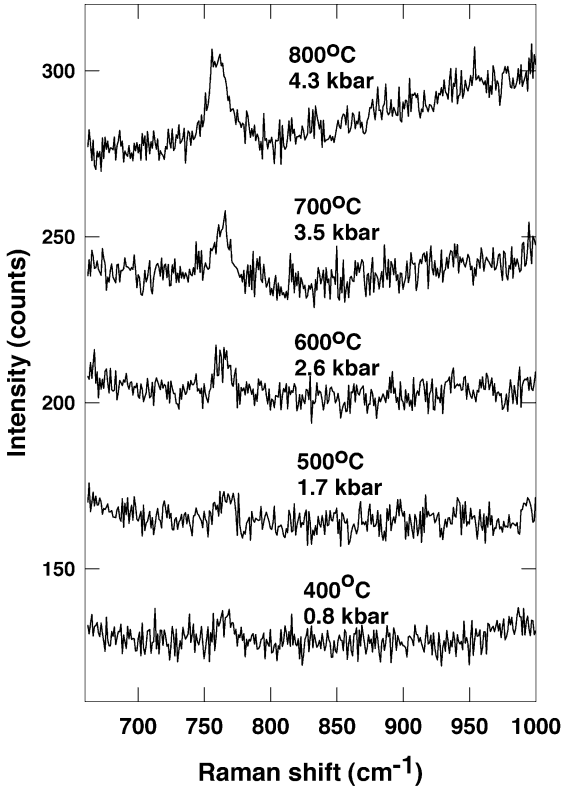

Fig. 1. Raman spectra of aqueous fluid in equilibrium with solid quartz. The homogenization temperature of the fluid is $T_H = 324 \pm 2$ °C ($\rho = 0.654$ g/cm^3). The spectra are shifted along the intensity axis for clarity.

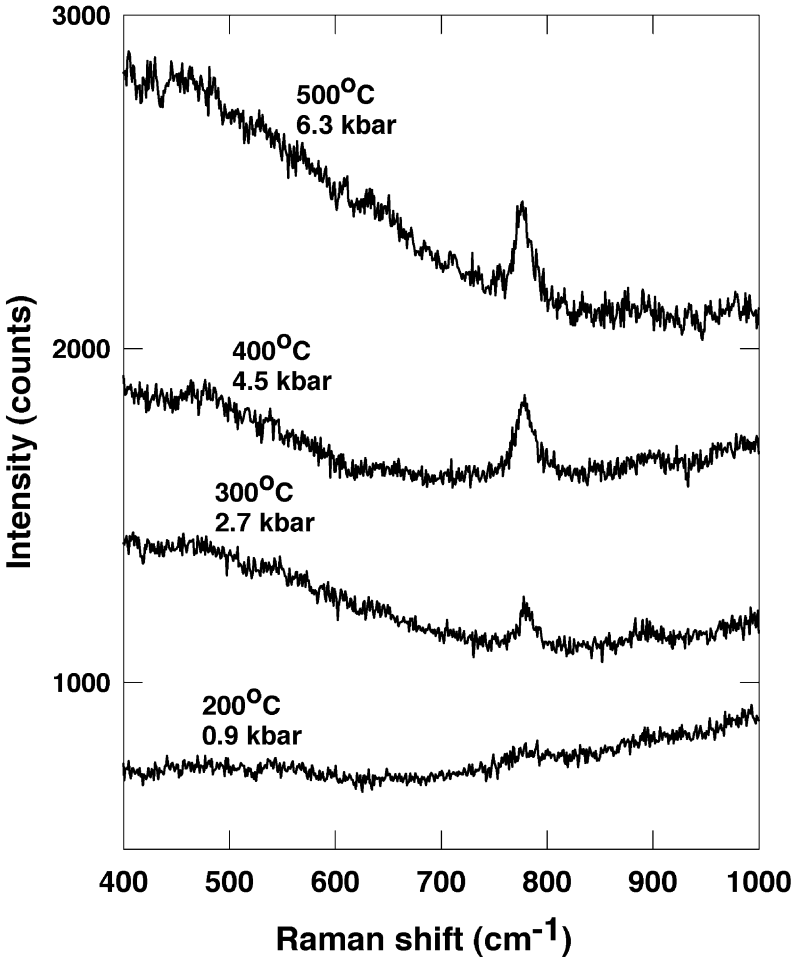

Fig. 2. Raman spectra of aqueous fluid in equilibrium with solid quartz. The homogenization temperature of the fluid is $T_H = 150 \pm 2$ °C ($\rho = 0.920$ g/cm^3). The spectra are shifted along the intensity axis for clarity.

exists in the solution, within the detection limit of the spectrometer.

Time-dependent measurements of the 780 cm^{-1} band at selected temperatures in the range from 400 to 600 °C show that the intensity of the peak remains practically constant within experimental error (Fig. 3). This implies that the equilibrium concentration of the corresponding species is reached very quickly (probably a few seconds after reaching the respective temperature). Similarly, the position of the peak at a given temperature and pressure remains practically the same (± 1.5 cm^{-1}) within the accuracy of the spectrometer. The observation that equilibrium is attained rapidly is consistent with kinetic data by Rimstidt and Barnes (1980) who have shown that the rate of silica dissolution strongly increases with temperature.

According to calculations of the frequencies and the relative Raman intensities of the normal modes of the H_4SiO_4 molecule (Zotov and Keppler, 2000 and references therein), the band at 760–780 cm^{-1} is due to the totally symmetric stretching mode of H_4SiO_4. In order to further confirm this band assignment, we also performed measurements on deuterated solutions and calculated the isotopic shifts of the normal modes for a fully deuterated D_4SiO_4 molecule using the same

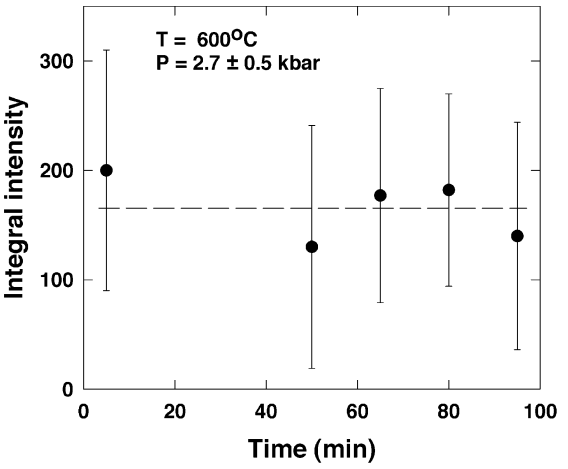

Fig. 3. Dependence of the integral intensity of the 780 cm^{-1} band on the delay time before the measurement at 600 °C for a fluid with $T_H = 324 \pm 10$ °C ($\rho = 0.654$ g/cm^3).

molecular geometry and force constants. The calculated isotopic shift of the 780 cm^{-1} mode of about 1.014 is in good agreement with the isotopic shift 1.009 ± 0.001 measured in a deuterated system (Fig. 4). This is additional evidence that the peak originates from H_4SiO_4 molecules. The difference between the observed and calculated isotopic shift of 780 cm^{-1} mode is probably due to the small difference in the density of the protonated ($\rho = 0.62$ g/cm^3) and the

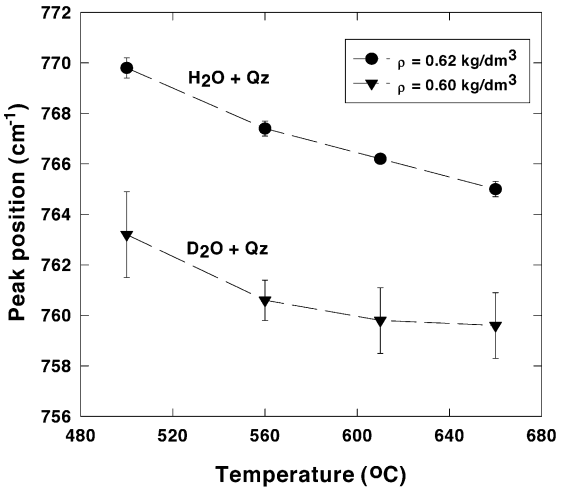

Fig. 4. Temperature dependence of the frequency of the 780 cm^{-1} mode of H_4SiO_4 in protonated (●) ($\rho = 0.62$ g/cm^3) and deuterated (▼) ($\rho = 0.60$ g/cm^3) fluids.

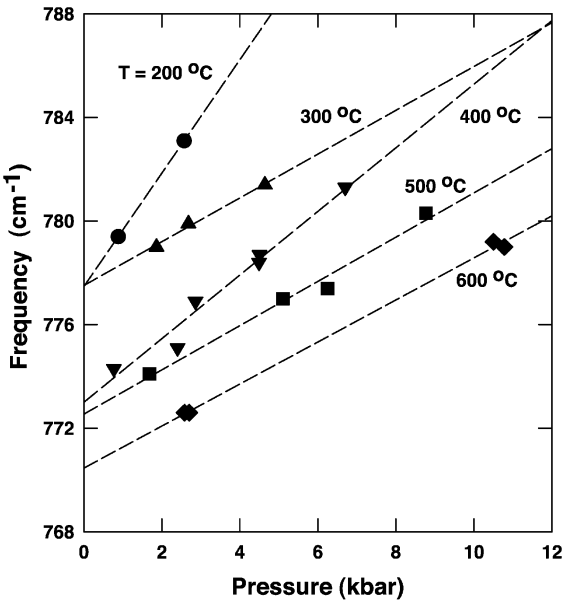

Fig. 5. Dependence of the frequency of the 780 cm^{-1} mode of H_4SiO_4 on pressure at different temperatures. The dashed lines are linear regression fits.

deuterated ($\rho = 0.60$ g/cm^3) solutions as well as to anharmonic effects which are not included in the potential model used.

The frequency of the 780 cm^{-1} mode shifts with temperature and pressure (see Fig. 5). We attribute these changes to anharmonic effects rather than to changes in the polymerization (as suggested by Alvarez and Sparks, 1985). At each temperature the data were fitted with the expression $v = v_o + a_P P$. The results of the fits are given in Table 1. The frequency of the 780 cm^{-1} mode increases with pressure for all temperatures due to compression of the Si–O bonds and corresponding increase of the Si–O stretching

Table 1
Linear regression coefficients $v = v_o + a_P P$ for the A_1 mode of H_4SiO_4 at different temperatures

T (°C)	v_o (cm^{-1})	Isobaric pressure derivative a_P (cm^{-1}/kbar)	r^2
200	777.5	2.19	–
300	777.5 ± 0.2	0.84 ± 0.08	0.9960
400	773.0 ± 0.5	1.23 ± 0.11	0.9841
500	772.5 ± 0.5	0.85 ± 0.08	0.9915
600	770.5 ± 0.2	0.81 ± 0.03	0.9989

force constant. However, the normal mode frequency at zero pressure v_0 as well as the isothermal pressure derivative decrease with temperature due to softening of the Si–O interactions.

At constant temperature the full width at half maximum increases approximately linearly with increasing pressure. This may indicate that the reorientational and vibrational relaxation times of the H_4SiO_4 molecules decrease with increasing pressure. The full widths at half maximum, extrapolated to constant pressure $P=1$ bar, increase almost linearly with temperature (Fig. 6a) and are linearly correlated with the decrease of the frequency of the 780 cm^{-1} band with temperature (Fig. 6b), in agreement with theoretical predictions including third-order anharmonicity (Liu Ming et al., 2000, and references therein).

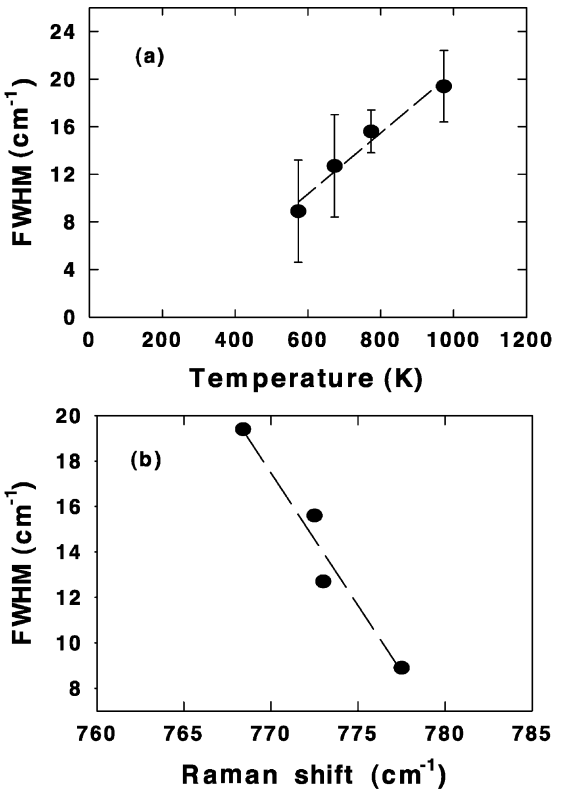

Fig. 6. (a) Dependence of the full width at half maximum (FWHM) of the 780 cm^{-1} mode of H_4SiO_4 on temperature, extrapolated to a reference pressure of 1 bar. The dashed line is a linear regression fit. (b) Correlation between the position and the FWHM of the 780 cm^{-1} mode of H_4SiO_4 at a reference pressure of 1 bar. The dashed line is a linear regression fit.

The similarity of the Raman spectra obtained from experiments with different bulk density indicates that, apart from the anharmonic broadening, the H_4SiO_4 molecules exist in the solution as well defined entities without significant distribution in bond lengths, bond angles and polarizability parameters. This implies that the concentration of the orthosilicic acid molecules is directly proportional to the intensity of the 780 cm^{-1} band. In the case of dilute solutions, concentration (moles of solute per volume of solution) and molality m (moles of solute per mass of solvent) are directly proportional to each other. In the following treatment, we prefer molality m as a measure of solution composition, as it allows direct comparison with the data on quartz solubility by Fournier and Potter (1982). Accordingly:

$$I = A(\mathrm{d}\sigma/\mathrm{d}\Omega)m, \quad (3)$$

where m is the molality in moles per kilogram, $\mathrm{d}\sigma/\mathrm{d}\Omega$ is the scattering cross-section of the molecules, which is proportional to the average square of the derivative of the molecular polarizability α with respect to the corresponding normal mode, and A is a geometric factor of the spectrometer system (McCreery, 1996). If the molality is a function of pressure and temperature, it can be determined from the intensity. In doing this, the pressure/temperature dependence of the polarizability derivatives is usually neglected. The solubility of quartz can be calculated at a given temperature and pressure using different empirical equations (Fournier and Potter, 1982; Manning, 1994). In the present study we have used the correlation equation of Fournier and Potter (1982), which is based on a larger set of experimentally measured solubility data. It is written in the form:

$$\log(m) = A(T) + B(T)\log(V) + C(T)(\log V)^2, \quad (4)$$

where m is the molality of dissolved silica, $A(T)$, $B(T)$, $C(T)$ are functions only of the temperature and V is the specific volume of pure water at a given pressure and temperature.

As we have seen, in the low-temperature/low-pressure regime only H_4SiO_4 species are observed within the detection limit of the present experiments. Therefore, m should be proportional to m_{H4SiO4}, and $\log(m)$

calculated from Eq. (4) should vary linearly with $\log(I_{H4SiO4})$, where I_{H4SiO4} is the integral intensity of the 780 cm^{-1} line of the H_4SiO_4 species corrected for frequency and thermal population effects by dividing with the thermal population factor $R = v^*(1 - \exp(-hcv/kT))$, where v is the frequency of the band, h is the Planck's constant, c is the speed of light in vacuum and k is the Boltzman constant. A typical $\log(m) - \log(I)$ plot is shown in Fig. 7. Note that it is difficult to obtain data for very small solubilities because the Raman intensity becomes very weak.

The fact that we observe a linear dependence between $\log(m)$ and $\log(I)$ indicates that (i) the scattering cross-section is practically independent of pressure and temperature under these conditions, and (ii) confirms that H_4SiO_4 molecules are the only species present up to 800 °C and 4.3 kbar at a bulk water density of 0.65 g/cm^3 and up to 500–600 °C and 6–8 kbar at a bulk density of 0.92 g/cm^3.

3.2. High-temperature/high-pressure regime

Fig. 8 shows the Raman spectra of a fluid with homogenization temperature $T_H = 230$ °C ($\rho = 0.82$ g/cm^3) up to 900 °C. A new broad band at about 630 cm^{-1} is observed above 600 °C together with much weaker bands at about 230, 370, 920 and 1100 cm^{-1}. These bands are particularly prominent in experiments where very high pressures are reached. The bands at 370 and 1050–1100 cm^{-1} may be partially due to vibrations of H_4SiO_4 (Zotov and Keppler, 2000), while the other bands must be due to some new silica species. Measurements of a fluid with $T_H = 67$ °C ($\rho = 0.98$ g/cm^3) at 950 °C show that a cross-over temperature/pressure exists above which the concentration of the H_4SiO_4 species starts to decrease at the expense of the newly formed polymerized species (Fig. 9).

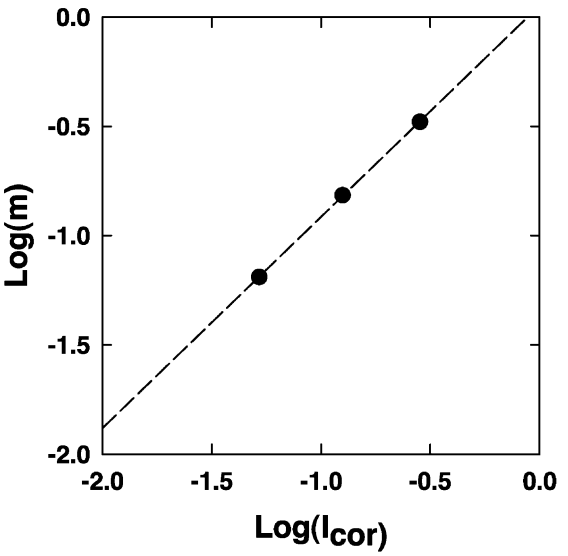

Fig. 7. Correlation of total silica molality and the corrected integral intensity of the 780 cm^{-1} mode of H_4SiO_4 in a fluid with $\rho = 0.99$ g/cm^3. The dashed line is a linear fit with $\log(m) = \log(I) + 0.0829$ and regression coefficient 0.9986. The errors in $\log(I)$ are ≤ 0.02.

Aside from H_4SiO_4, the simplest silica species one might expect in aqueous fluids is pyrosilicic acid $H_6Si_2O_7$. Calculated frequencies and relative Raman intensities of the $H_6Si_2O_7$ molecule (Zotov and Keppler, 2000) closely match the additional bands seen in the Raman spectra at high pressures and temperatures. The fact that we do not observe any other peaks with increasing temperature and pressure clearly demonstrates that $H_6Si_2O_7$ is the main polymerized species up to 950 °C and 15 kbar pressure. However, the FWHM of the 630 cm^{-1} band is much larger than the FWHM of the 780 cm^{-1} band of H_4SiO_4 and cannot be described by a single pseudo-Voigt function. This indicates that there is a distribution of $H_6Si_2O_7$ dimers with different Si–O–Si bridging and dihedral angle geometries. Moreover, we cannot exclude the formation of some protonated three-membered rings or the formation of some longer branched chains. The strongest Si–O peak of these species overlaps with the broad peak of the $H_6Si_2O_7$ dimers at about 630 cm^{-1} (Galeener, 1982; Kubicki and Sykes, 1993; Zotov et al., 1993). The latter oligomerization mechanism is favoured by the MD results of Garofalini and Martin (1994), according to which, at 650 K the polymerization of dimers species initially occurs via the formation of chains rather than via rings.

In order to investigate the effects of pressure and temperature on the polymerization reaction we have calculated the equilibrium constant of reaction (2). This constant is defined as:

$$K' = a_{H_6Si_2O_7} a_{H_2O} / a^2_{H_4SiO_4}, \quad (5)$$

where a_i is the activity of the respective species. Activities a_i are related to molar fractions x_i according

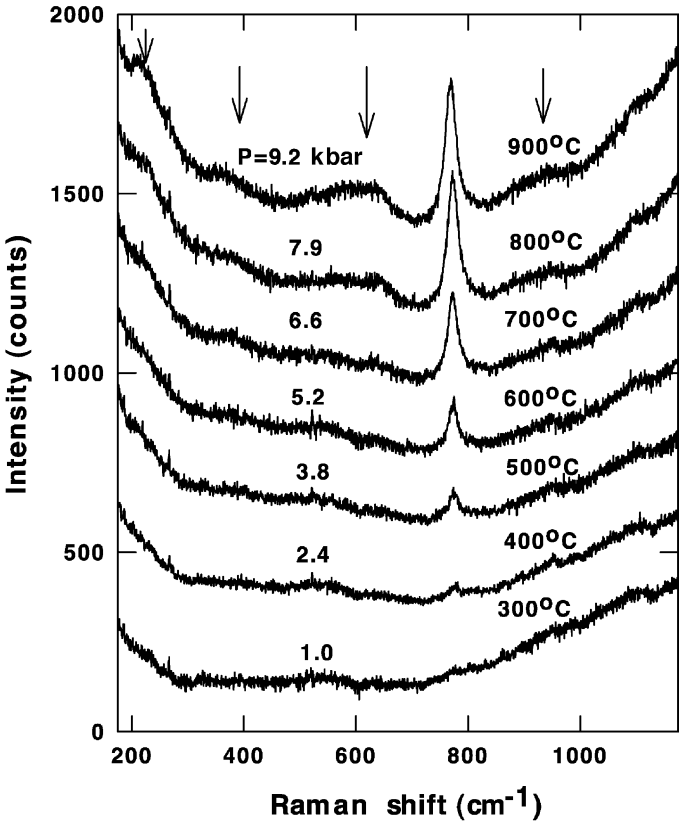

Fig. 8. Raman spectra of aqueous fluid in equilibrium with solid quartz. The homogenization temperature of the fluid is $T_H = 230$ °C ($\rho = 0.82$ g/cm^3). The spectra are shifted along the intensity axis for clarity. The arrows mark the position of the main $H_6Si_2O_7$ dimer peaks.

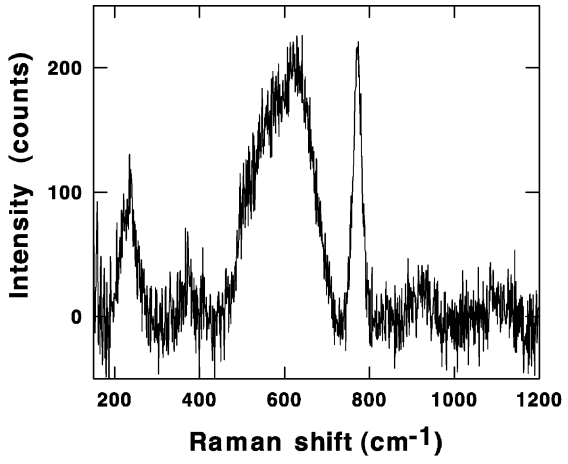

Fig. 9. Raman spectrum of aqueous fluid in equilibrium with solid quartz ($T_H = 67$ °C; $\rho = 0.98$ g/cm^3) measured at 950 °C. The background is subtracted for clarity.

to:

$$a_i = \gamma_i x_i, \tag{6}$$

where γ_i are the corresponding activity coefficients. Accordingly, Eq. (5) may be rewritten as:

$$K' = (\gamma_{H_6Si_2O_7}\gamma_{H_2O}/\gamma^2_{H_4SiO_4}) \times (x_{H_6Si_2O_7}x_{H_2O}/x^2_{H_4SiO_4}). \tag{7}$$

In the absence of independent data on activity coefficients, we assume in the following that the activity coefficients remain constant over the range of pressures and temperatures studied. Since we are dealing with mixtures of uncharged species at high temperatures, the activity coefficients are probably not far away from unity, similar to the situation in the system H_2O–CO_2 at high temperatures and pressures

(e.g. Kerrik and Jacobs, 1981). Therefore, the assumption of constant activity coefficients is not unreasonable. The chemical equilibrium in the fluid can then be described by a new equilibrium constant K based on molar fractions:

$$K = (x_{H_6Si_2O_7} x_{H_2O} / x^2_{H_4SiO_4}) \equiv K' (\gamma^2_{H_4SiO_4} / \gamma_{H_6Si_2O_7} \gamma_{H_2O}). \quad (8)$$

K is calculated assuming that the molalities $m_{H_4}SiO_4$ and $m_{H_6}Si_2O_7$ of the monomers and dimers are proportional to the integral intensities of the 780 and 630 cm^{-1} bands, divided by the corresponding scattering cross-sections (see Eq. (3)):

$$m_{H_4SiO_4} = A' \frac{I_{H_4SiO_4}}{d\sigma/d\Omega_{H_4SiO_4}} \quad (9)$$

and

$$m_{H_6Si_2O_7} = m_{H_4SiO_4} \frac{I_{H_6Si_2O_7}}{I_{H_4SiO_4}} \frac{d\sigma/d\Omega_{H_4SiO_4}}{d\sigma/d\Omega_{H_6Si_2O_7}}. \quad (10)$$

The integral Raman intensities were determined by numerical integration using the Lab208 Dilor software and corrected by the corresponding thermal population factors $R = \nu^*(1 - \exp(-hc\nu/kT))$ (see above). The scattering cross-sections $d\sigma/d\Omega_{H_4}SiO_4$ and $d\sigma/d\Omega_{H_6}Si_2O_7$ were taken equal to the corresponding reduced Raman intensities of the H_4SiO_4 and $H_6Si_2O_7$ molecules (10.9 and 5.5, respectively), which have been calculated previously (Zotov and Keppler, 2000). The constant A' in Eq. (9) (which is inversely proportional to the constant A in Eq. (3)) was determined by requiring that for each experiment, the calculated total molality of dissolved silica $m_{H_4}SiO_4 + m_{H_6}Si_2O_7$ at 600 °C should be equal to the total molality determined from the equation of Fournier and Potter (1982). Finally, the molar fraction of water in the fluid was calculated by assuming $x_{H_2}O + x_{H_4}SiO_4 + x_{H_6}Si_2O_7 = 1$. The equilibrium constants log$K$ for two representative experiments determined in this way are given in Table 2. The constant A' is equal to 0.218 for the data in Table 2a and 0.035 for the data in Table 2b. The standard deviations in the molalities, the molar fractions and the equilibrium constants are calculated by full-error propagation analysis.

The quartz solubilities calculated in this way are in very good agreement with the equation of Fournier and Potter (1982) up to 10–11 kbar (see Fig. 10). Beyond about 11 kbar, the equation of Fournier and Potter (1982) as well as the equation of Manning (1994) do not reproduce the molalities measured in the present study very well, probably because these empirical equations are not strictly valid beyond the P,T range for which they are calibrated ($P_{max} = 10$ kbar at 900 °C in both cases).

Table 2
Equilibrium constant of the reaction $2H_4SiO_4 = H_6Si_2O_7 + H_2O$

T (K)	P (kbar)	$I_{H_4}SiO_4$[a]	$I_{H_6}Si_2O_7$[b]	m (wt.%)[c]	$x_{H_4}SiO_4$[d]	$x_{H_6}Si_2O_7$[d]	$x_{H_2}O$[d]	log$K$[e]
(a) Bulk density $\rho = 0.94 \pm 0.06$ g/cm^3								
973	10.6 ± 2.3	0.60(3)	0.18(2)	3.49(19)	0.0066(3)	0.0040(5)	0.9894(23)	1.96(7)
1023	11.4 ± 2.3	0.75(4)	0.39(4)	5.53(37)	0.0084(4)	0.0086(11)	0.9830(47)	2.08(7)
1073	12.3 ± 2.5	0.98(5)	0.66(7)	8.35(61)	0.011(6)	0.0151(18)	0.9739(81)	2.07(7)
1123	13.2 ± 2.6	0.80(4)	0.95(10)	9.80(85)	0.0092(5)	0.0218(27)	0.9690(115)	2.40(7)
1173	14.0 ± 2.7	0.76(4)	1.25(12)	11.9(1.1)	0.0089(4)	0.0291(34)	0.9620(145)	2.55(6)
(b) Bulk density $\rho = 0.78 \pm 0.04$ g/cm^3								
973	5.6 ± 0.9	0.52(3)	0.078(8)	3.76(18)	0.0088(4)	0.0026(3)	0.9886(19)	1.52(7)
1023	6.2 ± 1.0	0.65(3)	0.117(11)	4.88(23)	0.0110(5)	0.0040(5)	0.9850(26)	1.51(7)
1073	6.8 ± 1.0	0.60(3)	0.159(16)	5.11(27)	0.0103(5)	0.0054(7)	0.9843(32)	1.70(6)

[a] Corrected integral intensities of the 780 cm^{-1} band of orthosilicic acid H_4SiO_4 monomers.
[b] Corrected integral intensities of the 630 cm^{-1} band of pyrosilisic acid $H_6Si_2O_7$ dimers.
[c] Total calculated molality in wt.%.
[d] Molar fractions of monomers, dimers, and water, respectively.
[e] K = equilibrium constant, see Eq. (8) in text. Standard deviations given in parantheses.

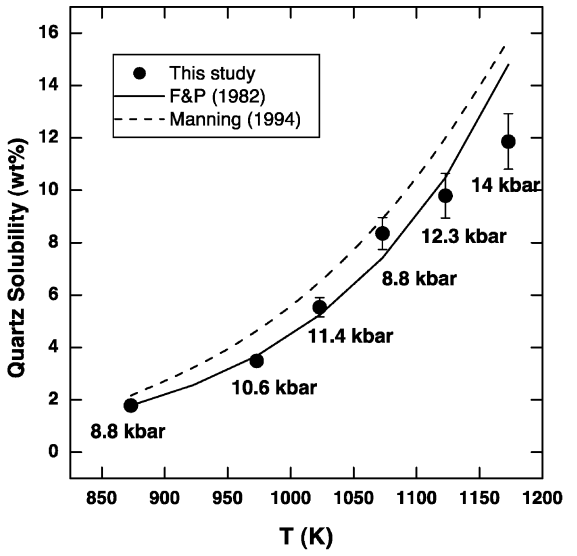

Fig. 10. Quartz solubility data (in wt.%) as a function of temperature for an isochoric experiment ($\rho = 0.94$ g/cm^3): Full line—calculation using the equation of Fournier and Potter (1982), dashed line—calculation using the equation of Manning (1994), ●—present study.

The dependence of the equilibrium constant on pressure can be described by the equation:

$$\ln K(P,T) = \ln K(P_0,T) - \frac{1}{RT}\int_{P_0}^{P} \Delta V_{sol} dP - \frac{1}{RT}\int_{P_0}^{P} V_{H_2O} dP, \quad (11)$$

where P_0 is some reference pressure and $\Delta V_{sol} = V_{H_6Si_2O_7} - 2V_{H_4SiO_4}$ is the change of the partial molar volume of the solute species.

Examination of the data demonstrates that in the pressure range where polymerization is observed (5–14 kbar), ΔV_{sol} is approximately independent of pressure. With this simplification, the expression for the equilibrium constant can be written as:

$$\ln K(P,T) = \ln K(P_0,T) - \frac{\Delta V_{sol}}{RT}(P - P_0) - \frac{1}{RT}\int_{P_0}^{P} V_{H_2O} dP. \quad (12)$$

The integral in Eq. (11) was calculated numerically with V_{H_2O} determined from the equation-of-state of water proposed by Saul and Wagner (1989).

Since $H_6Si_2O_7$ dimers are not observed below 5–6 kbar pressure, the reference pressure P_0 was set equal to 5 kbar. The molar volume of the solute ΔV_{sol} is practically independent of temperature and equal to $\Delta V_{sol} = -39 \pm 14$ cm^3/mol. The equilibrium constant K_0 at $P_0 = 5$ kbar as a function of temperature is shown in Fig. 11. The enthalpy of the polymerization reaction, calculated from the slope of this curve, is $\Delta H = 12.6 \pm 1.3$ kJ/mol and the entropy of the reaction ΔS, calculated from the intercept, is 40.7 ± 1.3 J/mol K.

The equilibrium constants of the polymerization reaction, calculated from Eq. (12), using the constants ΔV_{sol}, ΔH, and ΔS given above, are in excellent agreement with the measured values given in Table 2 (see Fig. 12). Calculations of the equilibrium constant of the polymerization reaction (2) at higher pressures using Eq. (12) show that it increases quickly with pressure at constant temperature, while the effect of increasing temperature at constant pressure is much smaller. In other words, pressure enhances strongly

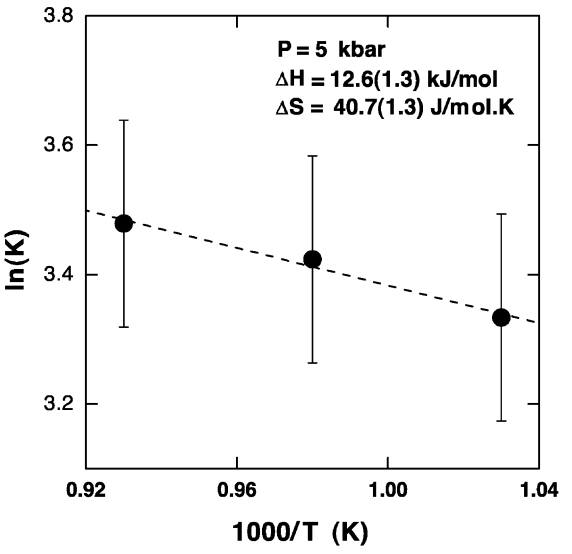

Fig. 11. Temperature dependence of the equilibrium constant K of the reaction $2H_4SiO_4 = H_6Si_2O_7 + H_2O$ at $P = 5$ kbar. The dashed line is a linear regression fit.

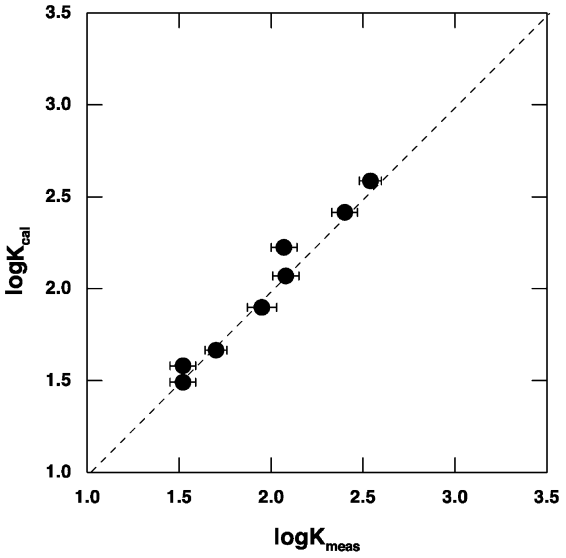

Fig. 12. Correlation between the calculated and measured equilibrium constant log(K) of the reaction $2H_4SiO_4 = H_6Si_2O_7 + H_2O$ for various pressures and temperatures. The dashed line is a linear regression fit with slope 1.

the formation of dimers and thus increases the solubility of quartz.

4. Conclusions

The present study demonstrates that Raman spectroscopy in externally heated diamond-anvil cells allows the identification of the major silica species dissolved in water in equilibrium with solid quartz. H_4SiO_4 monomers and $H_6Si_2O_7$ dimers are the main species in the fluid over the range of pressures and temperatures studied. The H_4SiO_4 monomers show little variation in bond lengths and bond angles, while the $H_6Si_2O_7$ dimers exhibit a significant Si–O–Si bridging angle and dihedral angle distribution. The quartz solubilities, calculated from our thermodynamic model, are in very good agreement with the equation of Fournier and Potter (1982). The polymerization reaction $2H_4SiO_4 = H_6Si_2O_7 + H_2O$ is strongly enhanced by the increase of pressure. The formation of polymerized species in the fluid explains the drastic increase of silica solubility under lower crustal and upper mantle P,T conditions. Ultimately, progressive polymerization will lead to a melt-like structure of the fluid and is therefore related to the onset of supercritical behaviour in the SiO_2–H_2O system (Kennedy et al., 1962). Thermodynamic models of silica solubility in water, which assume that H_4SiO_4 is the only species present, should not be used beyond the pressures and temperatures encountered in the upper part of the Earth's crust.

Acknowledgements

This work was supported by German Science Foundation (DFG Ke 501/2, Ke 501/3). We thank Harold Helgeson and an anonymous referee for their constructive criticism of a previous version of the manuscript. **MB**

References

Alvarez, R., Sparks, D.L., 1985. Polymerization of silicate anions in solutions at low concentrations. Nature 318, 649–651.

Anderson, G.M., Burnham, C.W., 1965. The solubility of quartz in supercritical water. Am. J. Sci. 263, 494–511.

Bass, J.L., Turner, G.L., 1997. Anion distribution in sodium silicate solutions: characterization by ^{29}Si NMR and infrared spectroscopies, and vapor phase osmometry. J. Phys. Chem. B 101, 10638–10644.

Bassett, W.A., Shen, A.H., Bucknum, M., Chou, I.M., 1993. A new diamond anvil cell for hydrothermal studies to 2.5 GPa and from – 190 °C to 1200 °C. Rev. Sci. Instrum. 64, 2340–2455.

Busey, R.H., Mesmer, R.E., 1977. Ionization equilibria of silicic acid and polysilicate formation in aqueous sodium chloride solutions to 300 °C. Inorg. Chem. 16, 2444–2450.

Cary, L.W., de Jong, B.H.W.S., Dibble Jr., W.E., 1982. A ^{29}Si NMR study of silica species in dilute aqueous solution. Geochim. Cosmochim. Acta 46, 1317–1320.

Dent Glasser, L.S., Lachowski, E.E., 1980. Silicate species in solution: Part 1. Experimental observation. Chem. Comm.-J.C.S. Dalton Ser., 393–402.

Dove, P.M., Rimstidt, J.D., 1994. Silica–water interactions. Rev. Mineral. 29, 259–308.

Earley, J.E., Fortnum, D., Wojcicki, A., Edwards, J.O., 1959. Constitution of aqueous oxyanions: perrhenate, tellurate and silicate ions. J. Am. Chem. Soc. 81, 1295–1301.

Feuston, B.P., Garofalini, S.H., 1990. Oligomerization of silica sols. J. Phys. Chem. 94, 5351–5356.

Fournier, R.O., Potter II, R.W., 1982. An equation correlating the solubility of quartz in water from 25 °C to 900 °C at pressures up to 10 kbars. Geochim. Cosmochim. Acta 46, 1969–1973.

Freund, E., 1973. Étude par spectroscopie Raman-laser des solutions aqueuses de silicates de sodium I. Résultats expérimentaux. Bull. Soc. Chim. Fr. 7–8, 2238–2243.

Galeener, F.L., 1982. Planar rings in vitreous silica. J. Non-Cryst. Solids 49, 53–62.

Garofalini, S.H., Martin, G., 1994. Molecular simulations of the polymerization of silicic acid molecules and network formation. J. Phys. Chem. 98, 1311–1316.

Greenberg, S.A., Sinclair, D., 1955. The polymerization of silicic acid. J. Phys. Chem. 59, 435–440.

Harris, R.K., Knight, C.T.G., 1983. Silicon-29 nuclear magnetic resonance studies of aqueous silicate solutions Part 5. First order patterns in potassium silicate solutions enriched in silicon-29. J. Chem. Soc., Faraday Trans. 79, 1525–1538.

Harris, R.K., Jones, J., Knight, C.T.G., 1980. Silicon-29 NMR studies of aqueous silicate solutions Part 2. Isotopic enrichment. J. Mol. Struct. 69, 95–103.

Hench, L.L., West, J.K., 1990. Molecular orbital models of silica. Annu. Rev. Mater. Sci. 25, 37–68.

Iler, R.H., 1979. The chemistry of silicaSolubility, Polymerization, Colloid and Surface Properties and Biochemistry. Wiley, New York.

Kennedy, G.C., Wasserburg, G.J., Heard, H.C., Newton, R.C., 1962. The upper three-phase region in the system SiO_2–H_2O. Am. J. Sci. 260, 501–521.

Kerrik, D.M., Jacobs, G.K., 1981. A modified Redlich–Kwong equation for H_2O, CO_2 and H_2O–CO_2 mixtures at elevated pressures and temperatures. Am. J. Sci. 281, 735–767.

Kinrade, S.D., Swaddle, T.W., 1988. Silicon-29 NMR studies of aqueous silicate solutions 1. Chemical shifts and equilibria. Inorg. Chem. 27, 4253–4259.

Knight, C.T.G., 1988. A two-dimensional silicon-29 NMR spectroscopic study of the structure of the silicate anions present in an aqueous potassium silicate solution. J. Chem. Soc., Dalton Trans., 1457–1460.

Kubicki, J.D., Sykes, D., 1993. Molecular orbital calculations of vibrations in three-membered alumosilicate rings. Phys. Chem. Miner. 19, 381–391.

Liu Ming, S., Bursill, L.A., Prawer, S., Beserman, R., 2000. Temperature dependence of the first-order Raman phonon line of diamond. Phys. Rev. B 61, 3391–3395.

Manning, C.E., 1994. The solubility of quartz in H_2O in the lower crust and upper mantle. Geochim. Cosmochim. Acta 58, 4831–4839.

McCreery, R.L., 1996. Instrumentation for dispersive Raman spectroscopy. In: Laserna, J.J. (Ed.), Modern Techniques in Raman Spectroscopy. Wiley, New York, pp. 41–72.

Rimstidt, J.D., Barnes, H.L., 1980. The kinetics of silica–water reactions. Geochim. Cosmochim. Acta 44, 1683–1699.

Saul, A., Wagner, W., 1989. A fundamental equation for water covering the range from the melting line to 1273 K at pressures up to 25 000 MPa. J. Phys. Chem. Ref. Data 18, 1537–1559.

Stumm, W., Morgan, J.J., 1981. Aquatic Chemistry, 2nd edn. Wiley Interscience, New York.

Walter, J.V., Helgeson, H.C., 1977. Calculation of the thermodynamic properties of aqueous silica and the solubility of quartz and its polymorphs at high pressures and temperatures. Am. J. Sci. 227, 1315–1351.

Zotov, N., Keppler, H., 2000. In-situ Raman spectra of dissolved silica species in aqueous fluids to 900 °C and 14 kbar. Am. Mineral. 85, 600–604.

Zotov, N., Michailova, B., Marinov, M., Konstantinov, L., 1993. Vibrational spectra of rings in silicate glasses—calculations on isolated structural units with topological disorder. Phys. A 201, 402–409.